ETA-PRODUCTION BY PHOTONS AND ELECTRONS*

B.H. Schoch

Physikalisches Institut,Universitaet Bonn, Germany

(Received June 25, 1993)

The experiments described in this contribution address the excitation of the nucleon in the second resonance region. The results of total cross section measurements with a tagged photon beam at energies close to the η-production threshold are reported.

PACS numbers: 14.40. Aq, 13.60. Le

1. Introduction

By using the beams of high duty factor electron accelerators precision experiments of exclusive reactions on the nucleon and the nucleus can be performed. Thereby, static properties like charge and current distributions, extracted via formfactor measurements, and electric and magnetic polarisibilities determined with photon scattering experiments, will be investigated. More dynamic properties can be studied by exciting the nucleon and the observation of the decay products. All experiments together will provide a data base for stringent tests of models of the nucleon. The experiments described in this contribution address the excitation of the nucleon in the second resonance region. Thereby, the detection of the η-meson allows to single out the S_{11}-resonance which couples very strongly to the η- N- channel. In performing exclusive experiments by exploiting the polarisation degrees of freedom the smaller amplitudes due to the other resonances and background terms can be extracted out of interference contributions. In the first part the results of total cross section measurements with a tagged photon beam at energies close to the η-productionn threshold will be reported [1]. In the second part data of total and differential cross sections of electro η-production will be presented.

---

* Presented at the Meson–Nucleus Interactions Conference, Cracow, Poland, May 14–19, 1993.

2. The total cross section p(γ, η)p close to the production threshold

Fig. 1 shows the total photoabsorption cross section up to 3. 5 GeV. The excitation of resonances determines up to E_γ=2 GeV the shape of the cross section. In the second resonance region the $D_{13}(1520)$- resonance dominates the total cross section. This resonance decays almost exclusively into the (π-N)-channel. It's coupling to the (η-N)-channel amounts to $\approx$ 0. 01. The $S_{11}(1535)$, however, hardly seen in the total absorption cross section couples strongly (. 5-. 6) to the (η-N)- channel and dominates the p(γ, η)-total cross section. Smaller amplitudes may arise from the $P_{11}(1440)$-resonance close to the production threshold, and from Born-and other background terms. Fig. 2 shows, schematically, the set-up of the experiment.

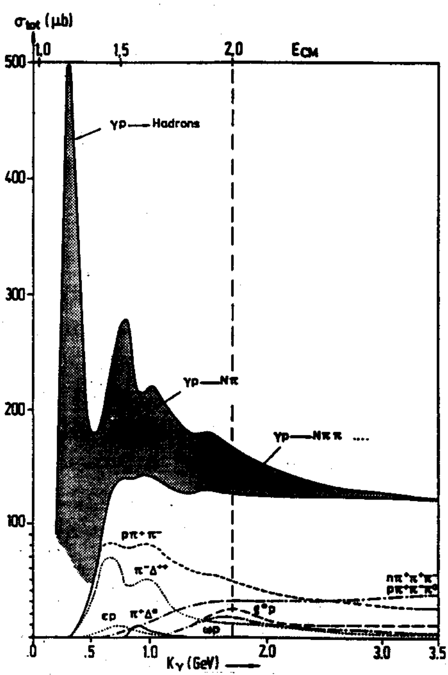

Fig. 1. Total absorption cross section for photons on the proton.

The electron beam from ELSA produces bremsstrahlung in a narrow cone at the radiator. The energy of the photon can be deduced by measuring the momentum of the electron which emitted the photon. Close to the threshold of the p(γ, η)-reaction the recoil protons are emitted in a narrow cone into the forward direction. These protons are measured in coincidence with the tagged bremstrahlung photon. Fig. 3 shows a missing mass plot of a data sample.

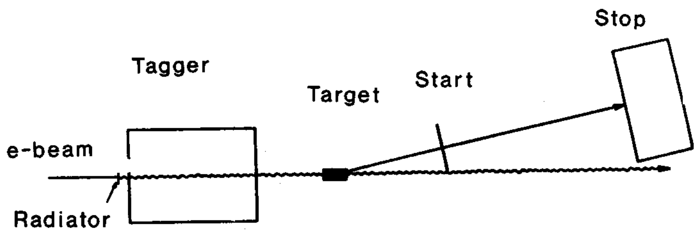

Fig. 2. A schematic view of the set-up used at ELSA.

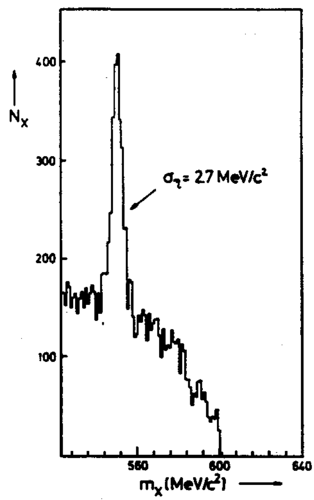

Fig. 3. Missing mass spectrum for the reaction $\gamma + p \rightarrow p + X$.

Close to the η-mass a peak stands up on top of a background which is due to two pion processes. Fig. 4 shows the total cross section as a function of energy. Shown with the data are the results of calculations with different assumptions [3]. The basis of the calculations are the graphs shown in Fig. 5. In addition to Born(a) and (b)- and resonance(c) and (d) graphs a graph(e) due to vector meson exchange in the t-channel has been added. Given the uncertainties of the input parameters in the calculations it is clear that -given precise-measurements of the total cross section are not enough to fix the relevant parameters, uniquely. Measurements of differential cross sections as well as polarisation observables are necessary in order to disentangle s-and -p-wave contributions. Measurements on the neutron allow a separation of the isoscalar contributions.

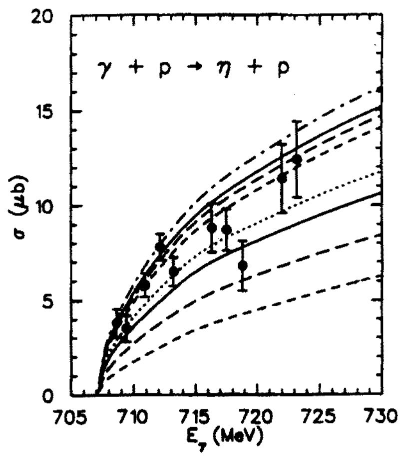

Fig. 4. Results of the measurement of the total cross section compared with calculations.

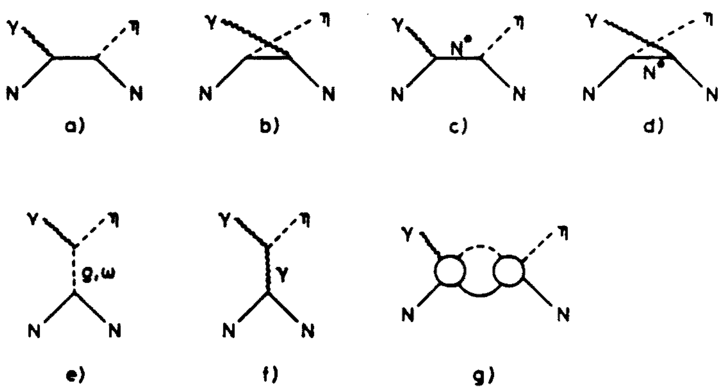

Fig. 5. The calculated graphs.

3. The results of a measurement p(e,e'η)p

Additional information can be gained by using an electron beam as a probe. Fig. 6 shows schematically the pieces of information which can be extracted from electron induced experiments. Starting with a current-current interaction the known-in complete experiments-4-vector potential describing the virtual photon provides a basis to project on the unknown properties of the hadronic object. Therefore, 3 basic properties as a function of energy and momentum transfer can be extracted out of the data: The distribution of charge, convection- and spin current. The experiment described here became possible because of the high duty factor beam of ELSA.

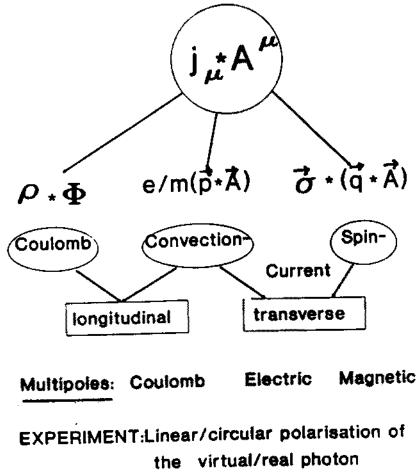

Fig. 6. The different projections upon the electromagnetic probe.

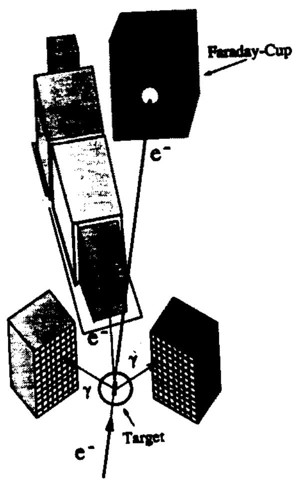

Fig. 7. Set-up for the electroproduction experiment.

The set-up is shown in Fig. 7 [2].
Two lead glass arrays of 88 detectors each served as photon detectors in singling out the two photon decay of the ETA-meson. Using the granularity of the detector and the pulseheight information the ETA-momentum was reconstructed. Fig. 8 shows recorded events by plotting the time spectra of the two blocks in the plane. A pronounced peak occurs where the electron and the two photons coincide in the overall time resolution interval of the triple coincidence. The scattered electron was measured with an electron spectrometer which has the rather large momentum acceptance of $\Delta p/p = \pm.12$. Therefore, a missing mass bin of $\Delta E \approx 120\,\text{MeV}$ could be covered

in one setting. Another advantage of such a configuration makes use of the fact that by detecting the ETA via it's two decay photons the whole angular range in θ_η as well as Φ_η could be covered in one setting. The corresponding efficiencies were determined by simulating the given set-up. The total cross section extracted from the data is shown in Fig. 9.

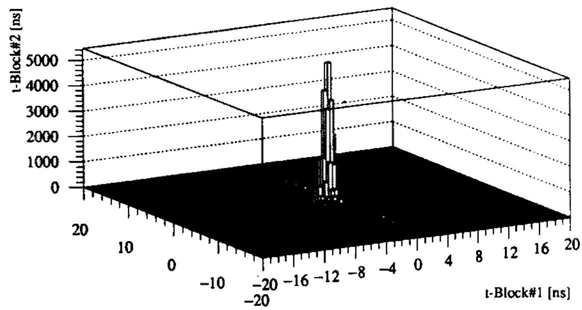

Fig. 8. Time of flight spectra measured in the two blocks.

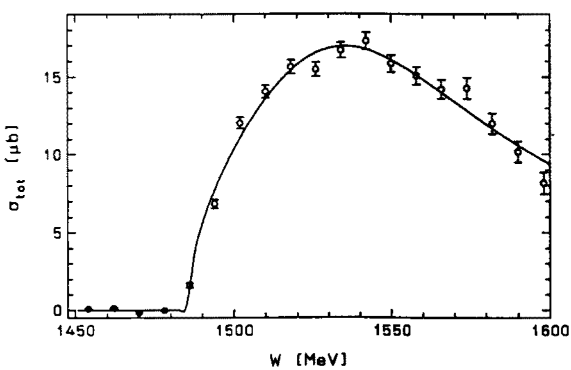

Fig. 9. Total cross section for the reaction p(e, e'η)p.

The curve is a result of a Breit–Wigner fit. Thereby, it has been assumed that the total cross section is totally determined by the S_{11}-resonance. In order to extract angular distributions the energy range shown in Fig. 9 was split into 6 energy intervals. The differntial cross sections for two of them are shown in Fig. 10.

The solid line is the result of a three parameter fit $d\sigma/d\Omega = a + b \cdot \cos\theta_\eta + c \cdot \cos^2\theta_\eta$. These are by no means constant distributions as anticipated if only the S_{11}-resonance dominates. Other resonances, especially, the d-wave resonance which should contribute to c as well as the background contributions are clearly visible. A further analysis including the results of

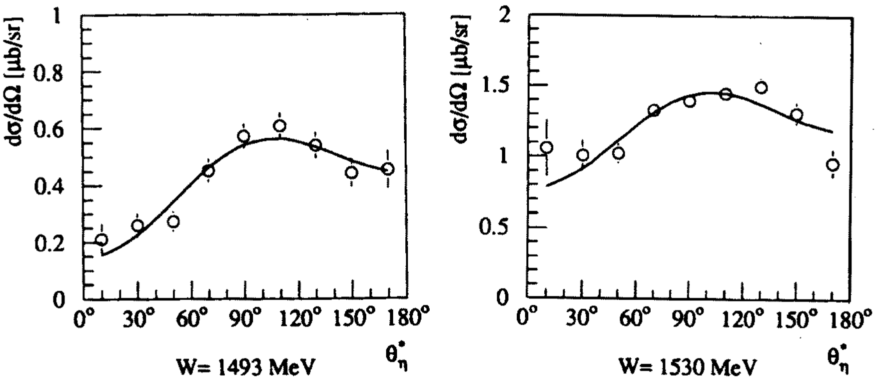

Fig. 10. **Differential cross sections close to threshold and on top of the S_{11}-resonance.**

the mesurement of the Φ_η -distribution which is in the very same set of data is in progress.

REFERENCES

[1] G. Anton, Habilitationsschrift, Univ. of Bonn, 1993, unpublished.
[2] M. Wilhelm, PhD-Thesis, Univ. of Bonn, 1993, unpublished.
[3] L. Tiator *et al.*, TRIUMF-Preprint, TRI-PP-92-47, 1992.